Percolation and conduction in restricted geometries

2000 J. Phys. A: Math. Gen. 33 1683

(http://iopscience.iop.org/0305-4470/33/8/312)

J. Phys. A: Math. Gen. **33** (2000) 1683–1692. Printed in the UK PII: S0305-4470(00)08605-4

Percolation and conduction in restricted geometries

P Lajkó†‡ and L Turban†

† Laboratoire de Physique des Matériaux, Université Henri Poincaré (Nancy I), BP 239, F–54506 Vandœuvre lès Nancy Cedex, France

‡ Institute of Theoretical Physics, Szeged University, H–6720 Szeged, Hungary

Received 11 October 1999

Abstract. The finite-size scaling behaviour for percolation and conduction is studied in two-dimensional triangular-shaped random resistor networks at the percolation threshold. The numerical simulations are performed using an efficient star–triangle algorithm. The percolation exponents, linked to the critical behaviour at corners, are in good agreement with the conformal results. The conductivity exponent, $t' = \zeta/\nu$, is found to be independent of the shape of the system. Its value is very close to recent estimates for the surface and bulk conductivity exponents.

1. Introduction

Since the paper of Cardy [1] we know that, at a second-order phase transition, the local critical behaviour can be influenced by the shape of the system. Furthermore, in the case of conformally invariant two-dimensional (2D) systems, the tools of conformal invariance can be used, at the critical point, to relate the local critical behaviour at a corner to the surface critical behaviour [2, 3]. The corner shape, which is scale invariant, leads to local exponents varying continuously with the opening angle. This marginal local critical behaviour has been indeed observed numerically for different systems (see [4] for a review) and, more recently, analytical results have been obtained for the Ising model [5–8].

In this paper, we present a numerical study of the critical behaviour of 2D random resistor networks with triangular shapes. This problem involves two sets of exponents, namely the percolation exponents and the conductivity exponents [9–11]. Although our main interest concerns the conduction exponents, our simulations allow us, as a by-product, to check the conformal predictions for the corner exponents of the percolation problem.

The percolation exponents are known exactly, both in the bulk and at the surface, through a correspondance with the limit $q \to 1$ of the q-state Potts model [12–14]. The conformal aspects of the critical percolation problem in finite geometries have been extensively studied in [15], following the work of [16]. Conformal invariance has been also verified in a transfer-matrix calculation of the surface percolation exponent, using the gap-exponent relation [17]. The critical behaviour at surface and corners has been considered in [18] where the conduction problem is addressed briefly.

A recent series expansion study [19] suggests that the surface conductivity has the same critical behaviour as the bulk one (see [20] and references therein). The main purpose of this paper is to examine, with high numerical accuracy, whether the shape of a finite system may have some influence on the scaling behaviour of the conductivity.

We study the finite-size-scaling behaviour of the conductance and percolation probability between points located at the corners of a triangle, either on the triangular or on the square

0305-4470/00/081683+10$30.00

lattice. As in the Lobb–Frank algorithm [21], the numerical technique involves a succession of triangle–star and star–triangle transformations, which allows one to reduce the triangular resistor network to a star network in a finite number of steps.

In section 2 we introduce the different correlation functions of the percolation and conduction problems and define the associated exponents. We also review the conformal results for the corner exponents. In section 3 we give a detailed explanation of the triangle–star star–triangle algorithm. The finite-size scaling simulation results are presented in section 4 and discussed in section 5.

2. Percolation and conduction correlation functions

We consider a random resistor network for which each lattice bond has a probability p to have a unit conductance and $1-p$ to be an insulator. Let the connectedness characteristic function c_{ij} be defined as

$$c_{ij} = \begin{cases} 1 & \text{if sites } i \text{ and } j \text{ are connected} \\ 0 & \text{otherwise.} \end{cases} \tag{2.1}$$

With $[\ldots]_{\mathrm{av}}$ denoting a configurational average, the percolation correlation function

$$P_{ij} = [c_{ij}]_{\mathrm{av}} \tag{2.2}$$

gives the probability that sites i and j belong to the same cluster of conducting bonds. The average conductance given by

$$G_{ij} = [g_{ij}]_{\mathrm{av}} \tag{2.3}$$

where g_{ij} is the conductance of the system between sites i and j, plays the role of a correlation function, or non-local conductive susceptibility, for the conduction problem [22]. Let N be the number of samples taken into account in the configurational average and N_{con} the corresponding number of samples for which sites i and j are connected. The correlation functions in equations (2.2) and (2.3) can be rewritten explicitly as

$$\begin{aligned} P_{ij} &= \lim_{N\to\infty} \frac{1}{N} \sum_{\alpha=1}^{N} c_{ij}^{\alpha} = \lim_{N\to\infty} \frac{N_{\mathrm{con}}}{N} \\ G_{ij} &= \lim_{N\to\infty} \frac{1}{N} \sum_{\alpha=1}^{N} g_{ij}^{\alpha} = \lim_{N\to\infty} \frac{N_{\mathrm{con}}}{N} \frac{1}{N_{\mathrm{con}}} \sum_{\alpha=1}^{N_{\mathrm{con}}} [g_{ij}^{\mathrm{con}}]^{\alpha}. \end{aligned} \tag{2.4}$$

Thus one can define the reduced conduction correlation function

$$\Gamma_{ij} = \frac{G_{ij}}{P_{ij}} = \lim_{N\to\infty} \frac{1}{N_{\mathrm{con}}} \sum_{\alpha=1}^{N_{\mathrm{con}}} [g_{ij}^{\mathrm{con}}]^{\alpha} \tag{2.5}$$

which gives the average conductance between two points i and j when they belong to the same percolation cluster.

In an infinite system, for two points at a distance $r_{ij} = r$, the correlation functions display a power law decay

$$P_{ij} \sim r^{-2x} \qquad \Gamma_{ij} \sim r^{-\zeta/\nu} \tag{2.6}$$

at the percolation threshold $p = p_{\mathrm{c}}$. The exponents x and ν are the scaling dimension of the bulk order parameter and the correlation length exponent for the percolation problem, respectively. The conductivity exponent ζ governs the behaviour of the macrosopic conductivity near the percolation threshold where [23]

$$\Sigma \sim (p - p_{\mathrm{c}})^{t} \qquad t = \nu t' = \zeta + (d-2)\nu \qquad p > p_{\mathrm{c}}. \tag{2.7}$$

Note that $\zeta/\nu = t'$ in two dimensions.

As mentioned in the introduction, the percolation exponents are exactly known in two dimensions through a correspondance with the q-state Potts model [24, 25]:

$$\nu = \tfrac{4}{3} \qquad x = \tfrac{5}{48} \qquad x_s = \tfrac{1}{3} \tag{2.8}$$

where x_s is the scaling dimension of the surface order parameter at the ordinary transition.

Recent high-statistics simulations led to the following accurate estimate for the conductivity exponent in two dimensions [20]:

$$t' = \frac{\zeta}{\nu} = 0.9825 \pm 0.0008 \qquad \zeta = 1.3100 \pm 0.0011. \tag{2.9}$$

Low-density series expansion results [19] are consistent with a surface conductivity exponent ζ_s keeping its bulk value ζ.

For a triangular-shaped system of size L, when the points i and j are located at corners with opening angles θ_i and θ_j, according to finite-size scaling, one expects the following behaviour at criticality:

$$\begin{aligned} P_{ij} &= P(\theta_i, \theta_j; L) \sim L^{-\eta(\theta_i,\theta_j)} \sim L^{-x(\theta_i)-x(\theta_j)} \\ \Gamma_{ij} &= \Gamma(\theta_i, \theta_j; L) \sim L^{-\zeta(\theta_i,\theta_j)/\nu}. \end{aligned} \tag{2.10}$$

Here $x(\theta_i)$ is the scaling dimension of the local order parameter at a corner with opening angle θ_i. In the following, we shall also consider the three-point correlation function P_{ijk}, which gives the probability that the points i, j and k, located at corners with opening angles θ_i, θ_j and θ_k, belong to the same cluster. This quantity scales like the product of the corresponding local order parameters, i.e. as

$$P_{ijk} = P(\theta_i, \theta_j, \theta_k; L) \sim L^{-\eta(\theta_i,\theta_j,\theta_k)} \sim L^{-x(\theta_i)-x(\theta_j)-x(\theta_k)} \tag{2.11}$$

at the percolation threshold.

A dependance of the local exponents on the opening angles is generally expected since a wedge is a scale-invariant geometry and the angles are marginal variables for the local critical behaviour. The critical 2D Potts model being conformally invariant, one obtains the local critical behaviour for the percolation problem at a corner using the conformal transformation $w = z^{\theta/\pi}$, which maps the half-space onto a wedge with opening angle θ [2, 3]. This leads to the following expression for the scaling dimension of the order parameter:

$$x(\theta) = \frac{\pi}{\theta} x_s. \tag{2.12}$$

3. The star–triangle transformation

Let us consider a finite random resistor network with the shape of an equilateral triangle of side L on the triangular lattice. Through a succession of triangle–star and star–triangle transformations, the original system can be progressively transformed into a star with three branches of length L as shown in figure 1.

At step p, in the first part of the lattice transformation, up-pointing triangles with coordinates (i, j) and bond conductances $g_\alpha^{(p)}(i, j)$ ($\alpha = 1, 2, 3$) are replaced by stars with bond conductances

$$\gamma_\alpha^{(p)}(i, j) = \frac{g_1^{(p)}(i, j)g_2^{(p)}(i, j) + g_2^{(p)}(i, j)g_3^{(p)}(i, j) + g_3^{(p)}(i, j)g_1^{(p)}(i, j)}{g_\alpha^{(p)}(i, j)} \qquad \alpha = 1, 2, 3 \tag{3.1}$$

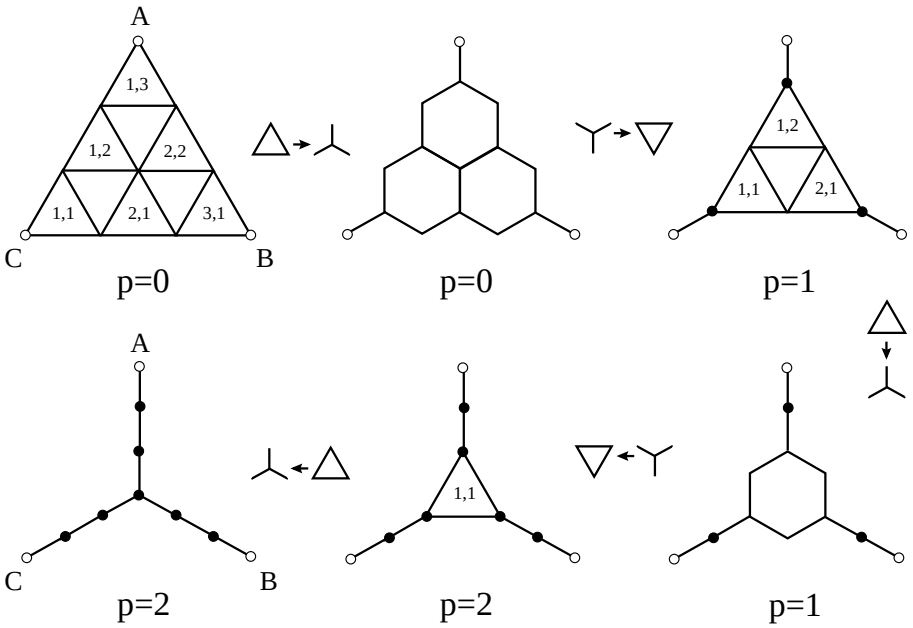

Figure 1. Reduction of a triangular-shaped system to a star through a succession of triangle–star and star–triangle transformations.

as shown in figure 2. In the second part, down-pointing stars are transformed into down-pointing triangles and up-pointing triangles are relabelled as indicated in figure 3. Thus one obtains the bond conductances for up-pointing triangles at step $p+1$ as

$$\begin{aligned} g_1^{(p+1)}(i,j) &= \frac{\gamma_2^{(p)}(i,j)\gamma_3^{(p)}(i+1,j)}{\gamma_1^{(p)}(i+1,j-1)+\gamma_2^{(p)}(i,j)+\gamma_3^{(p)}(i+1,j)} \\ g_2^{(p+1)}(i,j) &= \frac{\gamma_3^{(p)}(i,j+1)\gamma_1^{(p)}(i,j)}{\gamma_1^{(p)}(i,j)+\gamma_2^{(p)}(i-1,j+1)+\gamma_3^{(p)}(i,j+1)} \\ g_3^{(p+1)}(i,j) &= \frac{\gamma_1^{(p)}(i+1,j)\gamma_2^{(p)}(i,j+1)}{\gamma_1^{(p)}(i+1,j)+\gamma_2^{(p)}(i,j+1)+\gamma_3^{(p)}(i+1,j+1)}. \end{aligned} \tag{3.2}$$

Note that surface bonds in up-pointing triangles at step $p+1$ result from the transformation of incomplete down-pointing stars. The expressions given in (3.2) still apply in this case, provided the conductances associated with the missing bonds are set equal to zero, i.e. with the boundary conditions

$$\begin{aligned} &\gamma_1^{(p)}(i,0)=0 \qquad \gamma_2^{(p)}(0,j)=0 \qquad i,j=2,L-p \\ &\gamma_3^{(p)}(i,j)=0 \qquad i=2,L-p \qquad j=L-p-i+2. \end{aligned} \tag{3.3}$$

At step $p=L-1$, the final star configuration is obtained after the triangle–star transformation has been performed. Then, for example, the conductance between points A and B on a sytem with size L is given by

$$g_{AB}=\left[\sum_{p=0}^{L-1}\frac{1}{\gamma_1^{(p)}(1,L-p)}+\frac{1}{\gamma_2^{(p)}(L-p,1)}\right]^{-1}. \tag{3.4}$$

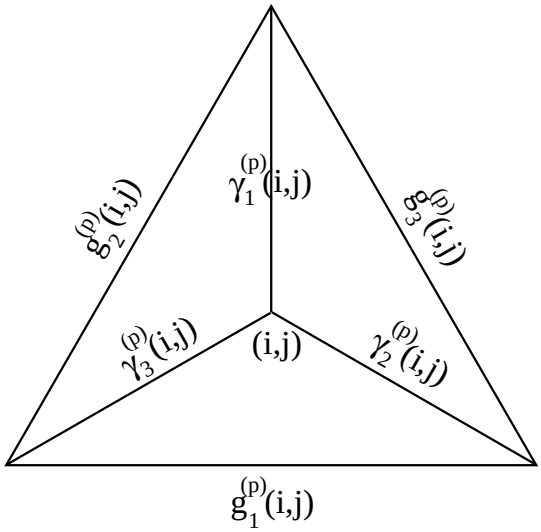

Figure 2. In the triangle–star transformation, up-pointing triangles with conductances $g_\alpha^{(p)}(i,j)$ are transformed into stars with conductances $\gamma_\alpha^{(p)}(i,j)$ given by equation (3.1).

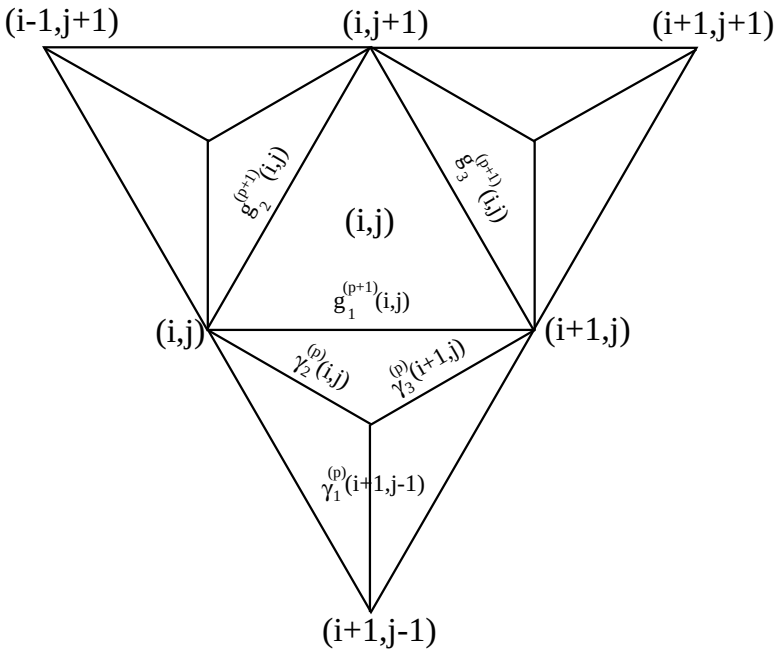

Figure 3. The conductances $g_\alpha^{(p+1)}(i,j)$ on up-pointing triangles at step $p+1$, given in equation (3.2), follow from star–triangle transformations on down-pointing stars. The conductances of the star involved in the construction of $g_1^{(p+1)}(i,j)$ are indicated. They originate from different up-pointing triangles at step p.

The same transformation, with all the conductances $g_3^{(0)}(i,j)$ set to zero in the initial configuration, can be used to reduce to a star a triangular-shaped system on the square lattice

as shown in figure 4.

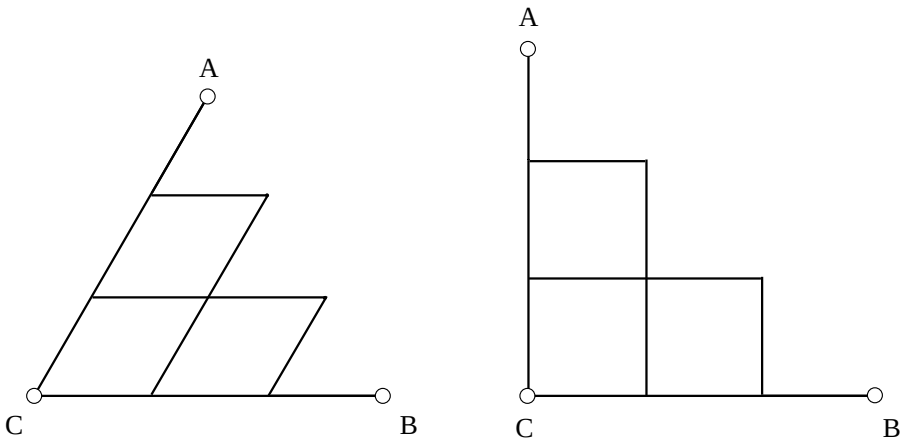

Figure 4. A triangular-shaped system on the square lattice is obtained through a deformation of the triangular lattice when the conductances are set to zero in one of the principal directions.

4. Finite-size scaling results

We have studied the finite-size scaling behaviour of the percolation and reduced conduction correlation functions between corners on triangular-shaped sytems. We worked at the percolation threshold, either on the triangular lattice ($p_c = 2\sin(\pi/18)$) or on the square lattice ($p_c = \frac{1}{2}$) [26].

On the triangular lattice (figure 1), we calculated the two-point functions $P(\frac{\pi}{3}, \frac{\pi}{3}; L)$, $\Gamma(\frac{\pi}{3}, \frac{\pi}{3}; L)$ and the three-point function $P(\frac{\pi}{3}, \frac{\pi}{3}, \frac{\pi}{3}; L)$ whereas on the square lattice (figure 4), we studied the two-point functions $P(\frac{\pi}{2}, \frac{\pi}{4}; L)$, $P(\frac{\pi}{4}, \frac{\pi}{4}; L)$, $\Gamma(\frac{\pi}{2}, \frac{\pi}{4}; L)$, $\Gamma(\frac{\pi}{4}, \frac{\pi}{4}; L)$ and the three-point function $P(\frac{\pi}{2}, \frac{\pi}{4}, \frac{\pi}{4}; L)$.

The initial bond configurations were generated using two types of random number generators, a simple shift register algorithm and the ranlux97 generator. We checked that both generators led to consistent results within the statistical errors. On the square lattice, in order to increase the number of percolating samples, the external bonds connecting A and B to the rest of the system in figure 4 were always assumed to be conducting.

We used system sizes of the form $L = 2^k$ up to $L = 256$. The star–triangle algorithm described in section 3 led to a computation time scaling roughly as $L^2 \ln L$. The number of samples generated was $N = 2 \times 10^7$ for the triangular lattice, except for the largest size where $N = 3 \times 10^7$. On the square lattice, 4×10^7 samples were generated for all sizes. The percolation and conduction correlation functions $P(L)$ and $\Gamma(L)$ were stored as n independent averages over groups of 10^6 samples in order to evaluate the statistical errors. More precisely, as defined in equation (2.5), the conduction correlation function is averaged over that part of the 10^6 samples for which the two points are connected.

Effective exponents at size L for the percolation and conduction problems were obtained using the two-points approximants

$$\eta_{\mathrm{eff}}(L) = \frac{\ln P(L/2) - \ln P(2L)}{\ln 4} \qquad \zeta/\nu|_{\mathrm{eff}}(L) = \frac{\ln \Gamma(L/2) - \ln \Gamma(2L)}{\ln 4}. \tag{4.1}$$

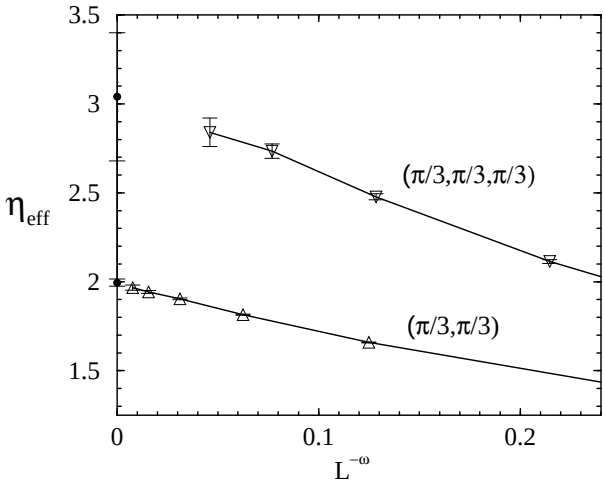

Figure 5. Percolation on the triangular lattice: effective decay exponents for the two-point (△) and three-point (▽) correlation functions plotted against $L^{-\omega}$ and their extrapolated values (●).

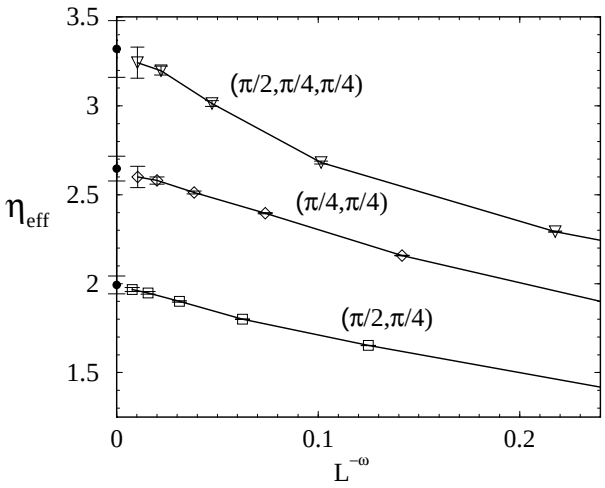

Figure 6. Percolation on the square lattice: effective decay exponents for the two-point (□, ◇) and three-point (▽) correlation functions plotted against $L^{-\omega}$ and their extrapolated values (●).

The central value of the approximants are calculated by averaging $P(L)$ and $\Gamma(L)$ over all the samples. The error bars were deduced from the mean-square deviations σ^2 of the approximants, obtained with the n statistically independent averages, as $\pm\sqrt{\sigma^2/(n-1)}$.

The finite-size results for the percolation exponents are shown in figure 5 for the triangular lattice and figure 6 for the square lattice. The results for the conductivity exponents are shown in figure 7 for both lattices.

The finite-size results were extrapolated in the following way. Assuming a single correction-to-scaling exponent ω, in each case we looked for the value of ω leading to the best linear variation at large size for the central value of the effective exponent as a function of $L^{-\omega}$. The intercept with the vertical axis gives the extrapolated values $\eta = \eta_{\rm eff}(\infty)$ and $\zeta/\nu = \zeta/\nu|_{\rm eff}(\infty)$. The statistical error on the extrapolated values were deduced, as above, from the

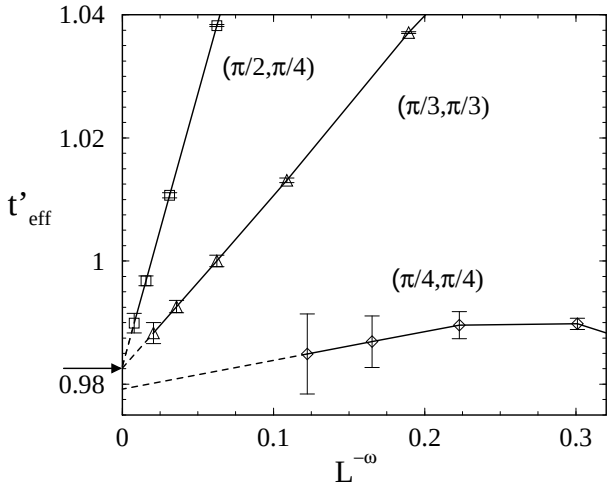

Figure 7. Conduction in triangular-shaped systems: effective decay exponents of the corner-to-corner conduction correlation functions on the triangular (△) and the square (□, ◇) lattices, plotted against $L^{-\omega}$. The dotted lines are the best linear fits used for the extrapolations and the arrow indicates Grassberger's result for the the bulk conductivity exponent.

Table 1. Exponents governing the decay of the percolation correlation functions (η) and the conduction correlation functions (ζ/ν) for triangular-shaped systems at criticality on the triangular and square lattices. The numerical values obtained for the percolation problem are compared to the values expected from conformal invariance. The last two lines give the effective correction-to-scaling exponents ω used in the extrapolation process.

	Triangular lattice		Square lattice		
Angles	$(\frac{\pi}{3}, \frac{\pi}{3})$	$(\frac{\pi}{3}, \frac{\pi}{3}, \frac{\pi}{3})$	$(\frac{\pi}{2}, \frac{\pi}{4})$	$(\frac{\pi}{4}, \frac{\pi}{4})$	$(\frac{\pi}{2}, \frac{\pi}{4}, \frac{\pi}{4})$
η numerical	1.99 ± 0.02	3.0 ± 0.3	2.01 ± 0.05	2.65 ± 0.07	3.32 ± 0.16
η conf. inv.	2	3	2	$\frac{8}{3}$	$\frac{10}{3}$
ζ/ν numerical	0.9827 ± 0.0017	—	0.9829 ± 0.0012	0.979 ± 0.018	—
ω percolation	1.05	0.76	1.14	1.06	1.13
ω conduction	0.81	—	0.43	1.02	—

mean-square deviation of the extrapolated exponents deduced from n statistically independent sets of approximants, taking the same value of ω for the linear fit. To the statistical error, we added a systematic error, linked to the deviation from the asymptotic regime. It was taken as the difference between the extrapolated values when one takes (or not) into account the largest size in the extrapolation process. Doing so, we probably overestimate the systematic error.

Due to the non-monotonous behaviour of the effective exponent for the conductance between corners with opening angle $\frac{\pi}{4}$, the error bar on the extrapolated exponent had to be estimated differently. It was obtained through an extrapolation of the extreme values of the effective exponents using the same method as for the central value.

The extrapolated exponents for the percolation and conduction problems are shown in table 1.

5. Discussion

Let us first consider the percolation problem. The decay exponents of the two- and three-point correlation functions, following from conformal invariance, are easily obtained using equations (2.8) and (2.10)–(2.12). Our numerical results in table 1 are in good agreement with the expected ones, although with a lower precision for the three-point exponents, due to larger statistical errors.

The percolation probability between two corners $P(\theta_i, \theta_j; L)$ can be written as the sum of two contributions. The leading one is the probability that i and j are connected without being connected to the third corner k which scales as $L^{-\eta(\theta_i,\theta_j)}$. The second is the probability that the three corners are connected and it decays as $L^{-\eta(\theta_i,\theta_j,\theta_k)}$. Thus we have a correction-to-scaling exponent equal to $x(\theta_k)$ for the two-point percolation probability. Another correction is due to the leading irrelevant operator with scaling dimension -1 at the surface [17]. This explains the value, close to 1, of the effective correction exponent ω for two-point percolation, since the amplitude of the first correction is small.

Our main result concerns the decay exponent ζ/ν which is equal to t' in two dimensions. The numerical values given in table 1 for the different geometries are all quite close to the value of t' for the bulk, which is given in equation (2.9). These results, together with the surface ones [19], strongly support the existence of a single conductivity scale, independent of the sample geometry. The influence of the opening angles can be seen in the amplitudes and perhaps also in the correction-to-scaling exponents.

One may notice that, apart from the case of the diagonal direction on the square lattice, the approximants for the conductivity exponents display a monotonous behaviour at large size. This is to be compared with the non-monotonous behaviour observed in [20] for bond percolation conductivity on the square lattice. It makes the extrapolation of the exponents more easy, thus reducing the computational effort necessary for a given precision on the extrapolated values.

Except for the diagonal direction on the square lattice, our error bars are about double those of Grassberger, for a maximum system size $L = 256$ instead of $L = 4096$ in [20]. If one accepts the universality of the conductivity exponent, which is strongly suggested by our results, the triangular geometry used here appears as a potentially efficient tool to further improve the precision on the value of ζ/ν.

Acknowledgments

The Laboratoire de Physique des Matériaux is Unité Mixte de Recherche CNRS No 7556. The authors are indebted to F Iglói for useful discussions. This work was supported by the Hungarian National Research Fund under grants Nos OTKA F/7/026004, M028418 and by the Hungarian Ministery of Education under grant No FKFP 0596/1999. PL thanks the Soros Foundation, Budapest, for a travelling grant.

References

[1] Cardy J L 1983 *J. Phys. A: Math. Gen.* **16** 3617
[2] Cardy J L 1984 *Nucl. Phys.* B **240** 514
[3] Barber M N, Peschel I and Pearce P A 1984 *J. Stat. Phys.* **37** 497
[4] Iglói F, Peschel I and Turban L 1993 *Adv. Phys.* **42** 683
[5] Abraham D B and Latrémolière F T 1994 *Phys. Rev.* E **50** R9
[6] Abraham D B and Latrémolière F T 1995 *J. Stat. Phys.* **81** 539
[7] Abraham D B and Latrémolière F T 1996 *Phys. Rev. Lett.* **76** 4813

[8] Davies B and Peschel I 1997 *Ann. Phys., Lpz.* **6** 187
[9] Kirkpatrick S 1973 *Rev. Mod. Phys.* **45** 574
[10] Bunde A and Havlin S 1991 *Fractals and Disordered Systems* (Berlin: Springer) p 97
[11] Stauffer D and Aharony A 1992 *Introduction to Percolation Theory* (London: Taylor and Francis) p 89
[12] Kasteleyn P W and Fortuin C M 1969 *J. Phys. Soc. Japan (Suppl.)* **26** 11
[13] Stephen M J 1977 *Phys. Rev.* B **15** 5674
[14] Wu F Y 1978 *J. Stat. Phys.* **18** 115
[15] Langlands R, Pouliot P and Saint-Aubin Y 1994 *Bull. Am. Math. Soc.* **30** 1
[16] Cardy J L 1992 *J. Phys. A: Math. Gen.* **25** L201
[17] de Queiroz S L A 1995 *J. Phys. A: Math. Gen.* **27** L363
[18] Wolf T, Blender R and Dietrich W 1990 *J. Phys. A: Math. Gen.* **23** L153
[19] Essam J W, Lookman T and De'Bell K 1996 *J. Phys. A: Math. Gen.* **29** L143
[20] Grassberger P 1999 *Physica* A **262** 251
[21] Lobb C J and Frank D J 1984 *Phys. Rev.* B **30** 4090
[22] Fish R and Harris A B 1978 *Phys. Rev.* B **18** 416
[23] de Gennnes P G 1976 *J. Physique Lett.* **37** L1
[24] Wu F Y 1982 *Rev. Mod. Phys.* **54** 235
[25] Cardy J L 1987 *Phase Transitions and Critical Phenomena* vol 11, ed C Domb and J L Lebowitz (New York: Academic) p 55
[26] Shante V K S and Kirkpatrick S 1971 *Adv. Phys.* **20** 325